Multiple PTOs in single OWC air chambers

Juan C. C. Portillo, Luís M. C. Gato, and João C. C. Henriques

Abstract—**The paper studies multi-PTO interactions in single-air chamber oscillating-water-column (OWC) wave energy converters (WECs). This approach seeks to i) tune the system's performance to sea states, ii) increase reliability through modular designs that are easier to install and replace, and iii) increase conversion efficiency through better matching between available power and electric conversion equipment. The strategy was assessed through a non-linear time-domain model for OWC WECs implemented in the multi-physics object-oriented language Modelica. The model is able to handle multiple PTOs, spring-like compressibility effects, and the hydrodynamic of OWC WECs. Different case studies considering two air turbines per air chamber for a fixed OWC show the proposed approach's versatility, constraints expected in real implementations, and potential pathways to overcome them. The wave-to-wire model considers air compressibility and non-linear power take-off systems, which is fundamental to assessing the damping level variation required for each incident wave condition. The cases presented are for one OWC of the Mutriku Wave Power Plant, but it is expected to be extensible for floating OWCs. Results under regular waves show a significant increase in power output in some wave periods (up to 300%), and control strategies are proposed for increasing power generation. This study represents an advance in the control strategies considering multiple PTOs for a single OWC air chamber to foster innovation actions.**

Index Terms—**Wave energy; Oscillating water column; Power take-off system control; Mutriku Wave Power Plant; Multi-PTO; Modelica.**

I. Introduction

THE European Commission set ambitious goals to reach carbon neutrality by 2050 [1]. According to European Union (EU) goals, ocean energy, such as wave and tidal energy systems and floating wind, shall reach about 40 GW by 2050 [2].

Wave energy technologies have yet to reach a commercial scale, but they continue evolving thanks to R&D efforts, especially in Europe, America and Asia. There is still no competitive levelised cost of energy (LCOE) for any of the wave energy systems known so far [3]. Nevertheless, public support initiatives have grown continually, especially due to the ambitious goals towards carbon neutrality and energy source diversification [4].

Oscillating water column (OWC) wave energy converters (WECs) have been studied extensively in recent decades [5]. Advancements in the associated technologies, such as the air turbines used as power take-off (PTO) systems and pilot projects already supplying electricity to local networks, are increasing the knowledge frontier to design, optimise, operate and maintain OWC WECs [6]–[8].

The industrialisation process necessary to boost a new industry sector, such as the future wave energy one, involves several political, technological, and organisational factors. Some factors related to the technological dimension are those associated with more efficient PTOs, better deployment strategies, increased reliability, modularity, and balance of systems thought for cost reductions, among others. This work focuses on better ways to deploy PTO for OWC WECs to increase their efficiency and devise new ways to design and optimise integrated systems.

This work aims to study the effect of using more than one PTO in one air chamber of an OWC WEC. This is achieved through a case study involving one air chamber of the Mutriku Wave Power Plant in Basque Country, Spain. Operational strategies using two biradial air turbines are presented for regular waves based on results from a time-domain model implemented in the object-oriented casual language Modelica. The next section presents the Mutriku Wave Power Plant. Afterwards, the numerical modelling approach is described, followed by the results. Finally, the main conclusions are highlighted.

II. Mutriku Wave Power Plant

The Mutriku Wave Power Plant (MWPP) comprises 16 OWC WECs. Each air chamber was designed to be equipped with an air turbine coupled to a generator. The original rated capacity of the turbo-generator set was set to 18.5 kW, with a total plant capacity of 296 kW. The original turbines used are of the Wells type [6], [9]. Nevertheless, other types of air turbines have been tested, such as the biradial air turbine designed at IST/ULisboa and Kymaner [10]. Fig. 1 shows the cross-section of one of the 16 air chambers.

The hydrodynamic coefficients that served as input to the time-domain numerical model described in Section III were obtained using the software WAMIT© version 7. A mesh considering five OWCs with 7736 source panels was used to obtain the hydrodynamic coefficients. The central OWC results were used for the time-domain simulation. Computations involved 320 regular wave frequencies for the heave degree of freedom of the OWCs, modelled as thin pistons. The bathymetry was considered a flat horizontal plane coincident with the plant's draft at the OWC opening side. The draft was set at a mean water level of 5.65 m.

J. C. C. Portillo (e-mail: juan.portillo@tecnico.ulisboa.pt), L. M. C. Gato (e-mail: luis.gato@tecnico.ulisboa.pt), and J. C. C. Henriques (e-mail: joaochenriques@tecnico.ulisboa.pt) are with IDMEC, Instituto Superior Técnico, Universidade de Lisboa, Av. Rovisco Pais 1, 1049-001 Lisbon, Portugal.

Digital Object Identifier:
https://doi.org/10.36688/ewtec-2023-394

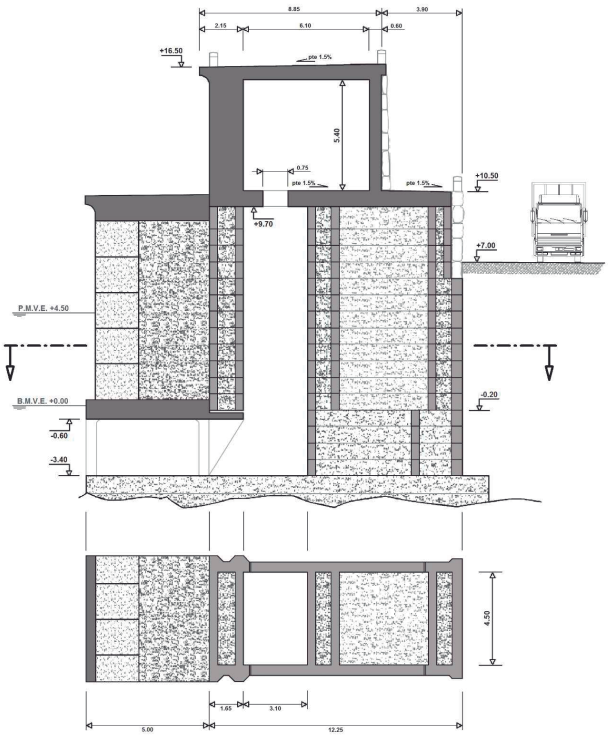

Fig. 1. Mutriku wave power plant dimensions [11].

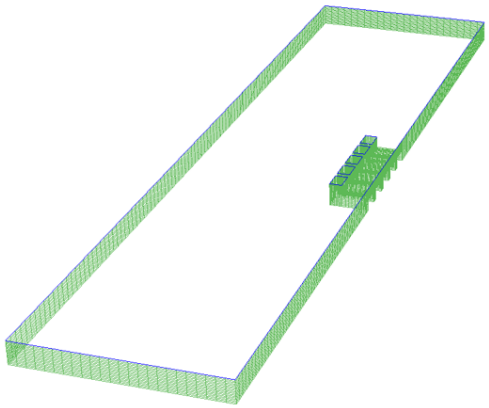

Fig. 2. Mesh representation of five OWCs of Mutriku wave power plant.

III. Numerical Modelling

This section introduces the theoretical modelling of the fixed OWC converter considered in this work. The water flow field is assumed incompressible and irrotational. The wave and piston-motion amplitudes are assumed much smaller than the typical wavelengths, which allows linear waterwave theory to be employed. The inner free-surface of the OWC is modelled as a thin rigid piston whose density is taken equal to water density and whose length parallel to the waves is much smaller than the wavelength.

The thin piston is assumed to oscillate only in heave (mode 9) while remaining horizontal. Modes of motion are represented by the vector $\mathbf{x}$, with time-dependent components x_i, where i is the mode index, which is $i = 9$ for the piston. In the absence of waves, it is $x_i = 0$ for any value of i. The equations of motion may be found in Ref. [12] for an arbitrary number of oscillating bodies and in Ref. [13] for the specific case of two bodies oscillating in heave, for example. The case considered here is simpler because it is considered only one hydrodynamic body, the rigid piston. Regarding the thin piston, only the components associated with heave modes are considered in the mass-inertia matrix M, corresponding to the piston's total mass (mass and added mass).

The time domain model considers air compressibility in the air turbine's pneumatic chamber and rotational speed control. The model was implemented in the object-oriented language Modelica, which has been verified for other cases through experimental data of a CD-OWC floating physical model at a scale of 1:40 [14].

A. OWC model: Equations of motion

The equation of motion for the rigid piston in heave (i=3) in time-domain, can be written as

$$(m_{99} + A^{\infty}_{99})\ddot{x}_9 + R_{99} + C_{99}x_9 = F_{e,p} - F_{\text{pto}}, \quad (1)$$

where x_j, $\dot{x}_j$, and $\ddot{x}_j$ are the displacement, velocity, and acceleration of the j-th mode. $M_{99} = m_{99} + A^{\infty}_{99}$ terms represent the mass and the added mass of the piston. C_{ij} represents the components of the hydrostatic coefficients matrix C.

Furthermore, the excitation forces $F_{\text{e},i}$ can be obtained as

$$F_{\text{e}}(t) = A_w(\omega_n)\,\Gamma(\omega_n)\,\cos\left(\omega_n t + \phi_r(\omega_n)\right), , \quad (2)$$

where ω_n is the wave frequency of the regular wave component n, $\Gamma_i(\omega_n)$ represents the exciting force or moment response, and $A_w(\omega_n)$ is the incident wave amplitude, both as functions of regular wave component with frequency ω_n. $\phi_r(\omega_n)$ is the excitation response phase to the wave component.

The radiation terms R_{ij} represent the convolution integrals considered as functions of the radiation damping coefficients and given by

$$R_{ij} = \int_0^t \kappa_{ij}(t-\tau)\,\dot{x}_j(\tau)\,\mathrm{d}\,\tau\,, \quad (3)$$

where,

$$\kappa_{ij}(t) = \frac{2}{\pi}\int_0^{\infty} B_{ij}(\omega)\cos(\omega t)\,\mathrm{d}\,\omega\,, \quad (4)$$

represents the radiation impulse response functions (IRFs). The convolution integral in Eq. (3) must be solved through direct integration or some other method. In this work, it was obtained using Prony's method formulation as presented in Ref. [15].

The $F_{\text{pto},i}$ term can be obtained from

$$F_{\text{pto}} = S_p\ p_{\text{ac}}(t), \quad (5)$$

where S_p and $p_{\text{ac}}(t)$ represent the piston water plane area and the instantaneous pressure in the air chamber, respectively. Nevertheless, the knowledge of the pressure within the chamber necessary to solve Eq. (5) requires solving simultaneously the complete system of equations which includes the definition of the air chamber, turbine, generator, and control models.

B. Air chamber model

The air in the pneumatic chamber is assumed to satisfy the ideal gas equation

$$\rho_{\text{ac}} = \frac{p_{\text{ac}}}{R\,T_{\text{ac}}}, \tag{6}$$

where ρ_{ac} is the density, p_{ac} is the pressure, T_{ac} is absolute temperature and R is the gas constant. Here, it is assumed that the process of turbulent and molecular diffusion is fast enough for the thermodynamic variables to be taken as spatially uniform in the air chamber.

The equation of continuity of mass may be expressed as [16]

$$-\dot{m} = \dot{\rho}_{\text{ac}}\,V + \rho_{\text{ac}}\,\dot{V}, \tag{7}$$

where V is the time-dependent volume of air in the chamber. Its time derivative $\dot{V}$ represents the volume flow rate displaced by the motion of the inner free surface (positive for upward motion). In the case of two turbines working at the same time in the air chamber, the total mass flow rate $\dot{m}$ equals the sum of the mass flow rate of both turbines, i.e. $\dot{m} = \dot{m}_{\text{t1}} + \dot{m}_{\text{t2}}$.

Since the air in the chamber is partly renovated at each wave cycle, the average temperature of the air in the chamber differs from the outer air temperature by no more than a few degrees Celsius (and much less than that in small model testing). This is why the heat exchanged across the chamber and turbine walls and at the inner air-water-free surface is very small compared with the work done by the inner free-surface motion or with the turbine work. It follows that the thermodynamic process that takes place in the inner air may be considered approximately adiabatic.

Because (i) air density is much smaller than water density, and (ii) the vertical size of the air chamber of a full-sized OWC does not exceed a few meters, differences in potential energy in the air chamber may be neglected [16].

The first law of thermodynamics allows the time-derivative of the internal energy $U(t)$ of air in the chamber to be written as

$$\frac{\mathrm{d}\,U}{\mathrm{d}\,t} = \begin{cases} -\dot{m}_{\text{out}}\,(h_{\text{out}} + \frac{1}{2}v_{\text{out}}^2) - p_{\text{ac}}\dot{V}, & \text{if } \; p_{\text{ac}} \geq p_{\text{at}} \text{ (ex.)} \\ \dot{m}_{\text{in}}(h_{\text{in}} + \frac{1}{2}v_{\text{in}}^2) - p_{\text{ac}}\dot{V}, & \text{if } \; p_{\text{ac}} < p_{\text{at}} \text{ (in.)} \end{cases}. \tag{8}$$

Here, h_{out} and h_{in} represent the specific enthalpy at the air chamber outlet during exhalation (ex.) and turbine outlet during inhalation (in.), respectively, and p_{at} is the atmospheric pressure. In the air chamber, no work is done on the fluid.

C. Power take-off modelling

The power take-off (PTO) system comprises air turbines driving electric generators. The control of their rotational speed is considered in the model. Each PTO is modelled as explained below.

1) Turbine modelling: The performance of the turbine is frequently presented in terms of dimensionless pressure head Ψ, dimensionless flow rate Φ, dimensionless power output Π and efficiency η_{turb} defined as (incompressible flow is assumed) (see [17], [18])

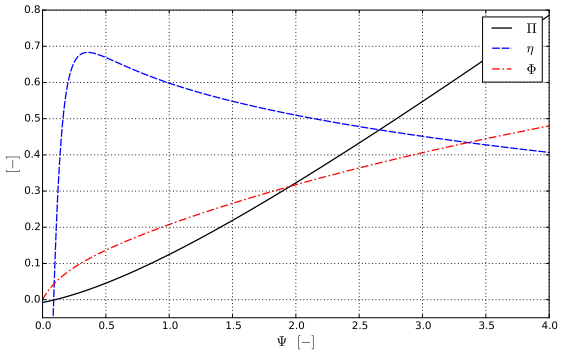

Fig. 3. Dimensionless flow rate, Φ, dimensionless power coefficient, Π, and efficiency, η, as functions of the dimensionless pressure head, Ψ, for the biradial air turbine [19], [20].

$$\Psi = \frac{\Delta p}{\rho_{\text{a,in}}\,\Omega^2\,d_{\text{t}}^2}, \tag{9}$$

$$\Phi = \frac{\dot{m}_{\text{turb}}}{\rho_{\text{a,in}}\,\Omega\,d_{\text{t}}^3} \tag{10}$$

$$\Pi = \frac{P_{\text{turb}}}{\rho_{\text{a,in}}\,\Omega^3\,d_{\text{t}}^5}, \tag{11}$$

$$\eta_{\text{turb}} = \frac{\Pi}{\Phi\,\Psi}. \tag{12}$$

Here, it is $\Delta p = p_{\text{at}}\,p^*$, where p^* is the dimensionless relative pressure oscillation in the chamber defined as

$$p^* = \frac{p}{p_{\text{at}}} - 1. \tag{13}$$

In Eqs. (9), (10) and (11), Ω is the turbine rotational speed (in radians per unit time), d_{t} is the turbine rotor diameter, $\dot{m}_{\text{turb}}$ is the turbine mass flow rate, and P_{turb} is the turbine power output.

The reference density $\rho_{\text{a,in}}$ is defined in stagnation conditions at the turbine entrance as

$$\rho_{\text{a,in}} = \begin{cases} \rho_{\text{ac}}, & \text{if } \; p^* > 0 \;\; \text{(ex.)} \\ \rho_{\text{at}}, & \text{if } \; p^* \leq 0 \;\; \text{(in.)} \end{cases}. \tag{14}$$

Figure 3 present the dimensionless flow rate Φ, dimensionless power coefficient Π, and efficiency η, as functions of the dimensionless pressure head, Ψ for a biradial air turbine.

The turbine aerodynamic power is computed from Eqs. (11) as

$$P_{\text{turb}} \;= \rho_{\text{a,in}}\,\Omega^3 d_{\text{t}}^5\,\Pi. \tag{15}$$

The mass flow rate of air through the turbine and the associated specific enthalpy are turbine outputs (see Figure 4). The specific enthalpy at the turbine's outlet $h_{\text{turb}}^{\text{out}}$ is defined as

$$h_{\text{turb}}^{\text{out}} = \begin{cases} h_{\text{ac}} - \left(\frac{p_{\text{ac}} - p_{\text{at}}}{\rho_{\text{a,in}}}\right)\eta_{\text{turb}}, & \text{if } \; p_{\text{ac}} \geq p_{\text{at}} \text{ (ex.)} \\ h_{\text{at}} + \left(\frac{p_{\text{ac}} - p_{\text{at}}}{\rho_{\text{a,in}}}\right)\eta_{\text{turb}}, & \text{if } \; p_{\text{ac}} < p_{\text{at}} \text{ (in.)} \end{cases}, \tag{16}$$

where h_{at} and h_{ac} are the atmospheric and air chamber-specific enthalpies, respectively.

2) Electric generator and control modelling: To maximize the turbine efficiency, it shall operate at the best efficiency point Ψ_{bep}, which implies that the turbine power should comply with [21]

$$P_{\text{turb}}\left(\Psi_{\text{bep}},\Omega\right) = \underbrace{\rho_{\text{a,in}}\, d_{\text{t}}^{5}\, \Pi\left(\Psi_{\text{bep}}\right)}_{a_{\text{bep}}=\text{const}}\, \Omega^{3}, \tag{17}$$

and the generator power control must follow the relation

$$P_{\text{ctrl}} = a_{\text{bep}}\Omega^{3}. \tag{18}$$

In a real OWC plant subject to irregular waves, the turbine rotational speed oscillates about a more-or-less averaged value, depending on the rotational inertia of the rotating elements and on the control strategy adopted for the counter torque $L_{\text{ctrl}} = P_{\text{ctrl}}/\Omega$ of the generator. A control law proposed in Ref. [21] relates the instantaneous generator's counter torque to the instantaneous rotational speed Ω as

$$L_{\text{ctrl}}\Omega = a\,\Omega^{b}, \tag{19}$$

where a and b are constants; the optimized dimensionless constant b usually takes a value about 3 [22], whereas constant a depends widely on turbine geometry and size.

3) The biradial turbine damping: The biradial turbine shows a relationship between dimensionless values of pressure head and flow rate that is fairly well-approximated by [10], [23]

$$\Psi = \mathcal{K}_{\text{tB}}\,\Phi^{2}, \tag{20}$$

where $\mathcal{K}_{\text{tB}}$ is a dimensionless constant, see Fig. 3b). From Eqs. (9) and (10) we get the biradial turbine damping

$$k_{\text{tB}} = d_{\text{t}}^{2}\left(\frac{\rho_{\text{a,in}}}{\mathcal{K}_{\text{tB}}\Delta p}\right)^{1/2}. \tag{21}$$

D. Time-domain implementation in OpenModelica

The time-domain model was implemented in OpenModelica, an open-source Modelica language-based modelling and simulation environment intended for industrial and academic usage [24]. The Modelica Language is a non-proprietary, object-oriented, equation-based language to conveniently model the dynamics of complex physical systems consisting of components (objects) [25]. These objects can be, for example, mechanical, electrical, electronic, hydraulic, thermal, control, electric power or process-oriented components. Modelica models are described by differential, algebraic, and discrete equations [26]. Modelica language-based environments have been used in many industries [25].

The implementation of the time-domain model described in Section III is depicted schematically in Fig. 4, in which the main objects and their principal connectors are shown for one OWC WEC. As Modelica is an equation-based language, each component is described by its corresponding set of equations and connectors (e.g. effort, flow, or stream variable's connectors)

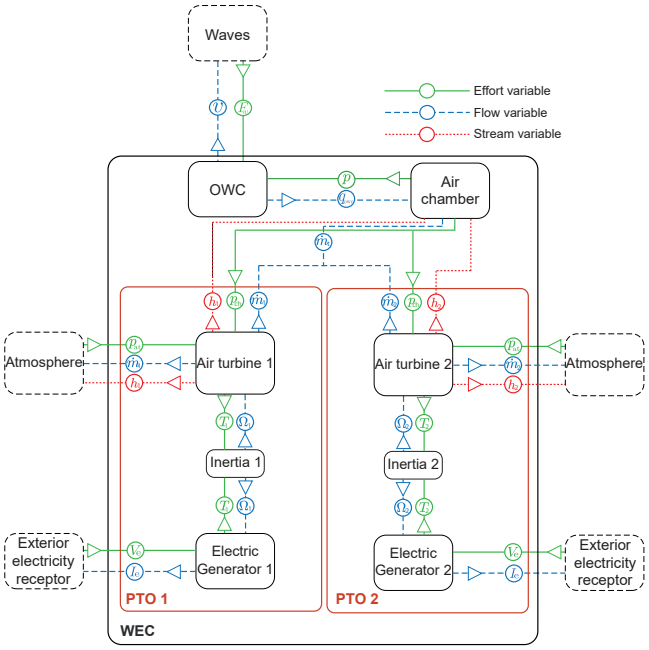

Fig. 4. Schematic representation of an OWC WEC and its connectors used in OpenModelica time-domain implementation.

that are used to establish the directions and interdependencies among the objects. OpenModelica was the open-source environment (editor) selected for the implementation, combined with a series of scripts in Python and C++.

Figure 4 shows two PTOs (1 & 2) connected to the same air chamber. The main effort connector variables chosen are forces, pressures, torques and voltages, while flow connector variables are velocities, volumetric flows, mass flows, rotational speeds, and current intensities. Specific enthalpy is a stream connector. The efficiency of the variable-frequency converter or other downstream electric/electronic systems were not considered in the present work. The electric generator losses were ignored. In addition, no viscous losses were considered in the results presented in this paper. Note that the specific enthalpies at turbines' output have been generically identified in Fig. 4 as h_1 and h_2 for each turbine, and they will take values according to the direction of the flow as presented in Eq. 16.

IV. Results

The numerical model presented was used to simulate different cases under regular waves of 2 m height and periods from 5 to 16 s. Cases comprised conditions using two turbines simultaneously, with the same and different diameters, and conditions using only one turbine. The objective was to determine operational strategies to increase the capture width ratio (CWR).

The CWR is defined as the ratio between the time-averaged pneumatic power ($\bar{P}$) and the time-averaged wave power per unit crest length ($\bar{P}_{\text{w}}$) multiplied by a selected characteristic length of one OWC of Mutriku Wave Power Plant ($D = 4.5$ m), as follows,

$$\text{CWR} = \frac{\bar{P}}{\bar{P}_{\text{w}} D}, \tag{22}$$

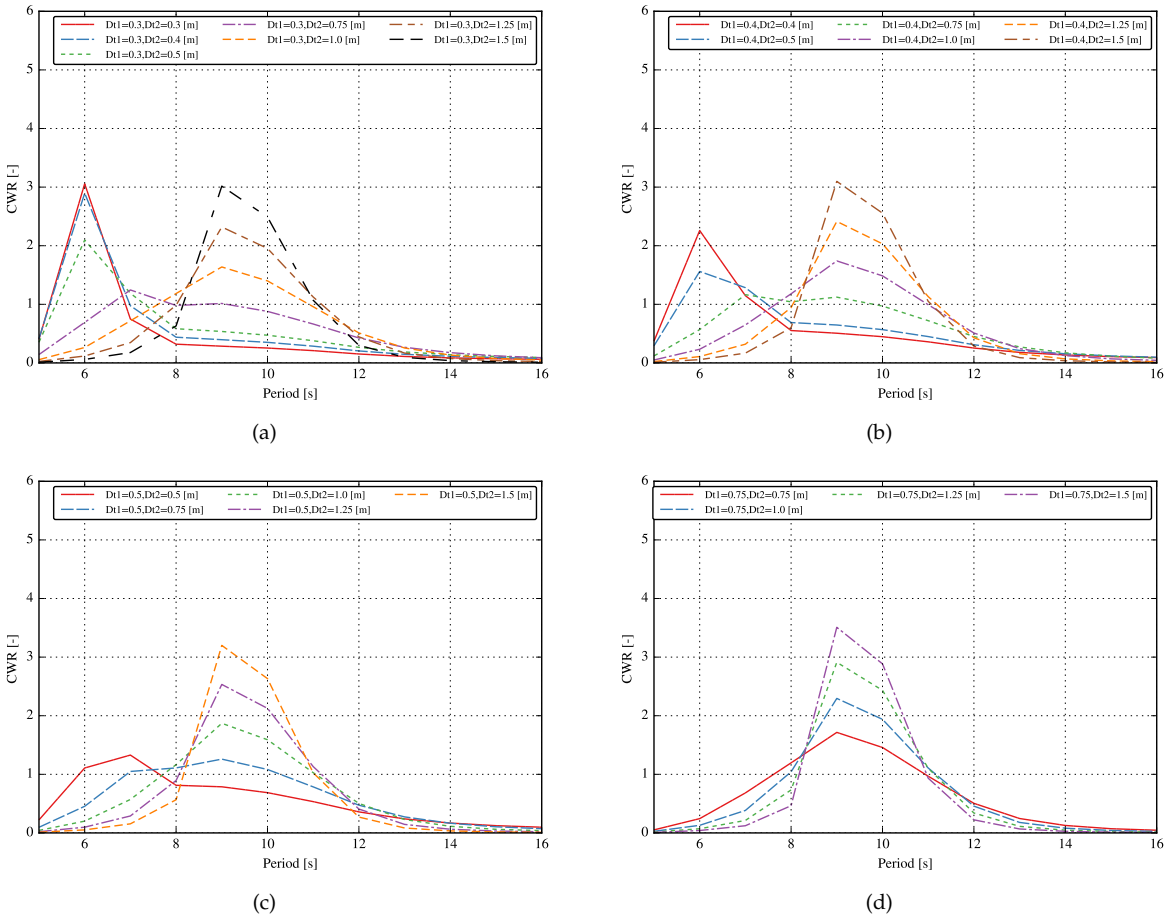

Fig. 5. Numerical results for the CWR under regular waves of height 2 m and different sets of two turbine rotor diameters in one air chamber. a) Smaller turbine rotor diameter of 0.3 m, b) Smaller turbine rotor diameter of 0.4 m, c) Smaller turbine rotor diameter of 0.5 m, and d) Smaller turbine rotor diameter of 0.75 m.

$\bar{P}$ is obtained from averaging the instantaneous power P.

Turbine rotor diameters for the biradial air turbine simulated were 0.3, 0.4, 0.5, 0.75, 1.0, 1.25, and 1.5 m. Results for the turbines working simultaneously are presented in Fig. 5. The figure shows that depending on the combination of the two turbine sizes connected to the air chamber, the maximum CWR occurs at different periods. It should be evident that the operational conditions for each turbine change depending on its size, resulting in different rotational speeds per turbine, pressure levels within the air chamber, and internal surface water elevation.

Figure 5 shows that the smaller turbine diameters perform better in terms of CWR for smaller periods (6-7 s), while turbines larger than 1.0 m perform better in period ranges from 8 to 12 s. From the numerical results, it was observed that depending on the period, one of the turbines might be responsible for most of the power output. Consequently, it might be convenient to think of operational strategies that consider one or two turbines working under conditions that have relative advantages in terms of power output.

An example of this operational strategy is shown in Fig. 6 for two biradial air turbines with rotor diameters of 0.4 and 0.75 m. For periods of 5 s to slightly before 7 s, having only the turbine with a rotor of 0.4 m is more effective than having the two turbines working simultaneously or having the largest turbine working alone (see Fig. 6(a)). Afterwards, until a period of 8 s, it is almost indifferent to set operating both turbines or only the largest turbine. Then, for periods greater than 8 s turning on both turbines increases the CWR until about 13 s, from where having the largest turbine working or both is indifferent. Applying this strategy in the example presented will increase the capture with ratio with regards to one turbine of rotor size of 0.75 m (the size of the Wells turbines installed in Mutriku Wave Power Plant) in more than 300% at 6 s, and in about 35% at 9 s, for example.

Furthermore, Fig. 6(b) presents the results of the OWC's heave response amplitude operator (RAO), for the same example, defined as OWC Heave RAO $= \bar{A}_{\text{owc}}/\bar{A}_{\text{w}}$, with $\bar{A}_{\text{owc}}$ and $\bar{A}_{\text{w}}$ being the mean amplitudes of the internal mass of water (OWC) and the waves, respectively. It can be observed that RAOs' highest values vary considerably depending on the turbine(s) working. The operational strategy modifies the OWC's hydrodynamic response. Regarding the dimensionless pressure $\hat{p}$, a considerable difference is observed for the smallest turbine working alone as expected due to the most significant restriction between the air chamber and the atmosphere. Also, the rotational speed is a consequence of the operational

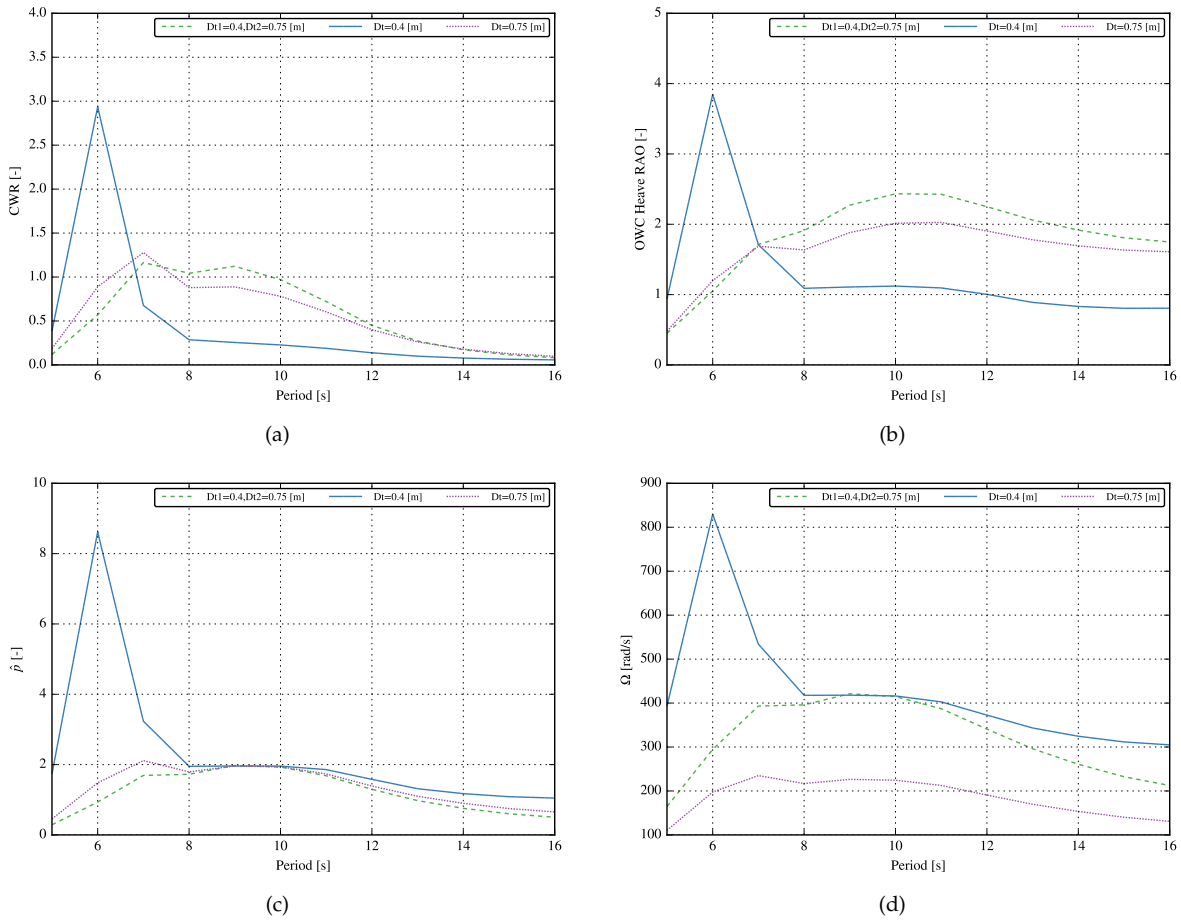

Fig. 6. Numerical results concerning only one turbine of rotor size 0.4 m, one turbine of rotor size 0.75 m and a case in which both turbines work simultaneously under regular waves of height 2 m. (a) CWR, (b) OWC Heave RAO, (c) dimensionless pressure ($\hat{p} = p/(\rho_w g A_w)$), and (d) rotational speed of the turbine. For the case of the two turbines working simultaneously, the rotational speed shown is the one for the smallest turbine, i.e. 0.4 m.

conditions and the rotational control law implemented to keep the turbine(s) working at its/their best efficiency point. Excessive rotational speed, like for the 0.4 m rotor diameter turbine working alone for a period of 6 s might be reduced through the rotational speed control at the expense of generating less power. This also depends on the constraints of the turbine itself and the generator.

The behaviour observed using two turbines in one air chamber and the strategy to switch on one or two turbines depending on the period of the waves seems to have a similar effect to varying the air chamber volume and the consequent variation of the spring-like compressibility effects, as presented in Ref. [27]. These compressibility effects also modify the OWC's hydrodynamics, resulting in shifts of CWR peaks in frequency and magnitude.

The capability to tune the OWC WEC to respond more efficiently to different wave conditions is of utmost importance in reducing the cost of energy, and incorporating two turbines to aid in this increase in mean annual power may be appealing for real deployments for various reasons. One of the reasons, as discussed before, is the increase CWR for a wider range of wave periods. A second reason is the increased operational flexibility, reliability, and availability of the system. For example, if one of the turbines fails, the other one might continue to operate until the corrective maintenance for the failed one happens. This increases reliability and availability, of course not at optimum or designed conditions, but it represents a gain. A third reason is the costs of the turbines; it might be the case that having two smaller turbines may be more cost-effective than having one larger turbine because the current costs of this type of turbine are high, and they usually increase to the cube of the mass. Furthermore, installation and maintenance costs might be another source of benefits due to the potentially smaller turbines and the consequent smaller equipment needed.

.

V. Conclusions

This work aimed to study the effects of using two impulse turbines, of the biradial type, at the Mutriku Wave Power Plant, as a strategy to increase power generation. The study comprised time-domain simulations using a numerical model implemented in the non-casual object-oriented programming language Modelica, which considers compressibility in the air chamber and rotational speed control of the turbines.

Simulations for combinations of turbine sizes between 0.3 and 1.5 m of rotor diameter under regular waves were performed. Results were presented in terms of CWR, and through an example of the implementation of the strategy for a selected case with turbines of 0.4 and 0.75 m rotor diameters. Results show that there might be significant gains in terms of CWR due to a better tunning of the OWC's hydrodynamics according to the wave periods. Besides the potential gains in power output, some other benefits might be associated with such a deployment strategy. Some of them are related to energy cost reductions, increased reliability and availability, and maintenance actions.

Future work will be focused on irregular wave conditions and the analysis of the mean annual power, levelised cost of energy computations, and effective numbers of turbines for various OWC WEC designs. Other types of turbines are also intended for further studies.

ACKNOWLEDGEMENT

The work was supported by the Portuguese Foundation for Science and Technology (FCT) through IDMEC, under LAETA, project UIDB/50022/2020.

REFERENCES

[1] European Commission, "The European Green Deal," 2022. [Online]. Available: https://eur-lex.europa.eu/legal-content/EN/TXT/?uri=CELEX:52019DC0640

[2] EC, "Boosting offshore renewable energy for a climate neutral Europe," 2020. [Online]. Available: https://ec.europa.eu/commission/presscorner/detail/en/ip_20_2096

[3] IEA-OES, "Annual Report: An Overview of Ocean Energy Activities in 2022," 2023. [Online]. Available: https://www.ocean-energy-systems.org/publications/oes-annual-reports/document/oes-annual-report-2022/

[4] European Commission, "The EU Blue Economy Report 2022," 2022. [Online]. Available: https://op.europa.eu/en/publication-detail/-/publication/156eecbd-d7eb-11ec-a95f-01aa75ed71a1

[5] A. F. O. Falcão and J. C. C. Henriques, "Oscillating-water-column wave energy converters and air turbines: A review," *Renewable Energy*, vol. 85, pp. 1391–1424, 2016.

[6] Y. Torre-Enciso, I. Ortubia, L. I. López de Aguileta, and J. Marqués, "Mutriku wave power plant: from the thinking out to the reality," in *Proc 8th European Wave Tidal Energy Conf, Uppsala, Sweden*, 2009, pp. 319–329. [Online]. Available: https://tethys.pnnl.gov/sites/default/files/publications/Torre-Enciso_et_al_2009.pdf

[7] A. F. O. Falcão, A. J. N. A. Sarmento, L. M. C. Gato, and A. Brito-Melo, "The Pico OWC wave power plant: Its lifetime from conception to closure 1986–2018," *Applied Ocean Research*, vol. 98, p. 102104, 2020.

[8] WAVENERGY, "WAVENERGY's projects and events," 2019. [Online]. Available: https://www.wavenergy.it/portfolio/

[9] P. Vigars, K. Lee, S. Shin, B. Ekergard, M. Leijon, Y. Torre-Enciso, D. Marina, and D. Greaves, "Project development," in *Wave and Tidal Energy*, D. Greaves and G. Iglesias, Eds. Hoboken, NJ: Wiley, 2018, pp. 533 – 586.

[10] A. A. D. Carrelhas, L. M. C. Gato, J. C. C. Henriques, A. F. O. Falcão, and J. Varandas, "Test results of a 30 kW self-rectifying biradial air turbine-generator prototype," *Renewable and Sustainable Energy Reviews*, vol. 109, pp. 187 – 198, 2019.

[11] EVE, "TD2 - TurboWave Challenge Descriptive Document. TURBOWAVE Project. Report for Innovation Procurement Call." 2022.

[12] J. Falnes, *Ocean Waves and Oscillating Systems: Linear Interactions Including Wave-Energy Extraction*. Cambridge: Cambridge University Press, 2002.

[13] J. Falnes, "Wave-energy conversion through relative motion between two single-mode oscillating bodies," *Journal of Offshore Mechanics and Arctic Engineering*, vol. 121, no. 1, pp. 32–38, 1999.

[14] J. C. C. Portillo, J. C. C. Henriques, L. M. C. Gato, and A. F. O. Falcão, "Model tests on a floating coaxial-duct OWC wave energy converter with focus on the spring-like air compressibility effect," *Energy*, p. 125549. , 2022.

[15] J. C. C. Henriques, J. C. C. Portillo, W. Sheng, L. M. C. Gato, and A. F. O. Falcão, "Dynamics and control of air turbines in oscillating-water-column wave energy converters: Analyses and case study," *Renewable and Sustainable Energy Reviews*, vol. 112, pp. 571 – 589, 2019.

[16] A. F. O. Falcão and J. C. C. Henriques, "The spring-like air compressibility effect in oscillating-water-column wave energy converters: Review and analyses," *Renewable and Sustainable Energy Reviews*, vol. 112, pp. 483 – 498, 2019.

[17] S. L. Dixon and C. A. Hall, *Fluid Mechanics and Thermodynamics of Turbomachinery*, 7th ed. Oxford: Butterworth-Heinemann, 2013.

[18] E. Dick, *Fundamentals of Turbomachines*, ser. Fluid Mechanics and Its Applications. Springer Netherlands, 2015.

[19] W. K. Tease, J. Lees, and A. Hall, "Advances in oscillating water column air turbine development," in *Proceedings of the 7th European Wave and Tidal Energy Conference*, Porto, Portugal, 2007.

[20] L. M. C. Gato, A. A. D. Carrelhas, F. X. C. da Fonseca, and J. C. C. Henriques, "OPERA deliverable D3.2 - turbine-generator set laboratory tests in variable unidirectional flow," Instituto Superior Técnico, Tech. Rep., 2017. [Online]. Available: http://opera-h2020.eu/wp-content/uploads/2016/03/OPERA_D3-2_Dry_Testing_IST.pdf

[21] A. F. O. Falcão, "Control of an oscillating-water-column wave power plant for maximum energy production," *Applied Ocean Research*, vol. 24, no. 2, pp. 73 – 82, 2002.

[22] A. A. D. Carrelhas and L. M. C. Gato, "Reliable control of turbine–generator set for oscillating-water-column wave energy converters: Numerical modelling and field data comparison," *Energy Conversion and Management*, vol. 282, p. 116811, 2023.

[23] L. M. C. Gato, A. A. D. Carrelhas, and A. F. A. Cunha, "Performance improvement of the axial self-rectifying impulse air-turbine for wave energy conversion by multi-row guide vanes: Design and experimental results," *Energy Conversion and Management*, vol. 243, p. 114305, 2021.

[24] OpenModelica, "OpenModelica: Introduction," Accessed on 02/03/2023. [Online]. Available: https://www.openmodelica.org/

[25] Modelica Association, "Modelica language," Accessed on 02/03/2023. [Online]. Available: https://www.modelica.org/modelicalanguage

[26] M. Otter and D. Winkler, "Modelica overview," Accessed on 02/03/2023. [Online]. Available: https://www.modelica.org/education/educational-material/lecture-material/english/ModelicaOverview.pdf

[27] J. C. C. Portillo, L. M. C. Gato, J. C. C. Henriques, and A. F. O. Falcão, "Implications of spring-like air compressibility effects in floating coaxial-duct OWCs: Experimental and numerical investigation," *Renewable Energy*, vol. 212, pp. 478–491, 2023.